NOT FOR
PUBLIC RELEASE

ERRATUM

Interlaminar Damage Model for Polymer Matrix Composites

PROOF ONLY

PAOLO LONETTI
Department of Structural Engineering
University of Calabria
Cosenza, Italy

EVER J. BARBERO*
Mechanical and Aerospace Engineering
West Virginia University
Morgantown, WV 26506-6106

RAFFAELE ZINNO
Department of Structural Engineering
University of Calabria
Cosenza, Italy

FABRIZIO GRECO
Department of Structural Engineering
University of Calabria
Cosenza, Italy

The publishers would like to apologize for the errors that occurred in the journal issue Vol. 37, Issue 16, pp. 1485–1504.

Equations (1) and (2) should have appeared as

$$D_i = \sum_{i=1}^{3} d_i n_i \otimes n_i \tag{1}$$

where $\otimes$ denotes the dyad product of tensors [25], n_i are the orthogonal principal directions, which in the proposed model coincide with the fiber, matrix, and thickness directions, d_i are the eigenvalues of the D tensor, which represents the damaged area ratio along the n_i directions. The dual variable of the damage tensor is the integrity tensor Ω,

Author to whom correspondence should be addressed. E-mail: ebarbero@wvu.edu

0021-9983/0?/00 0001–2 $10.00/0 DOI: 10.1177/0021998302042699
© 200? Sage Publications

which represents the undamaged area ratio. By the spectral decomposition theorem [11], the integrity tensor in the principal direction assumes the following form

$$\Omega_i = \sum_{i=1}^{n} \bar{\omega}_i (n_i \otimes n_i) \tag{2}$$

The use of damage and integrity tensors describes a mapping between the effective $\bar{c}$ and damaged c configurations by a linear operator f, as $f : c \to \bar{c}$. By the square root theorem [11], a unique transformation connects the damage and integrity tensor $\Omega = \sqrt{I - D}$. The integrity tensor is always symmetric and positive, because the net area reduction must be positive definite during damage evolution [2].

Equation (6) should have appeared as

$$\overline{\sigma} = M^{-1}(D)\sigma = \left(\sqrt{I-D} \otimes \sqrt{I-D}\right)^{-1} \sigma \overline{\varepsilon_e} = M(D)\varepsilon_e = \left(\sqrt{I-D} \otimes \sqrt{I-D}\right)\varepsilon_e \tag{6}$$

By the energy equivalence hypothesis [12–14], it is possible to define Hooke's law in the effective $\bar{c}$ and damaged c configurations as

Equation (28) should have appeared as

$$[K_{epd}][\Delta \underset{\sim}{u}] = [\Delta F]$$

PROOF ONLY

Journal of Composite Material, Vol. 37, n.16/2003.

Title: "INTERLAMINAR DAMAGE MODEL FOR POLYMER MATRIX COMPOSITES"

Authors: *P. Lonetti, E.J. Barbero, R. Zinno, and F. Greco.*

ERRATA

page 1486: *Equation (1) substitute* $\boldsymbol{D} = \sum_{i=1}^{3} d_i \boldsymbol{n}_i \otimes \boldsymbol{n}_i$ *for* $\boldsymbol{D} = \sum_{i=1}^{3} d_i \boldsymbol{n}_i \varepsilon\, \boldsymbol{n}_i$

page 1487, line 1: *Substitute the phrase* "where $\otimes$ denotes the dyad product of tensors" *for* "where ε denotes the dyad product of tensors"

page 1487: *Equation (2) substitute* $\boldsymbol{\Omega} = \sum_{i=1}^{3} \omega_i \boldsymbol{n}_i \otimes \boldsymbol{n}_i$ *for* $\boldsymbol{\Omega} = \sum_{i=1}^{3} \omega_i \boldsymbol{n}_i \varepsilon\, \boldsymbol{n}_i$

page 1487, line 8: *Substitute the phrase*
"The use of damage and integrity tensors describes a mapping between the effective $\overline{\mathbb{C}}$ and damaged $\mathbb{C}$ configurations by a linear operator *f*, as $f : \mathbb{C} \rightarrow \overline{\mathbb{C}}$."
for
"The use of damage and integrity tensors describes a mapping between the effective and damaged configurations by a linear operator f, as $f : c \rightarrow \overline{c}$."

Page 1487: Substitute *Equation (4).5*

$$\overline{\sigma}_{13} = \frac{1}{(F_{11}F_{22}F_{33})}[F_{11}]^{1/2}\sigma_{13}[F_{33}]^{1/2} = \overline{\sigma}_{31} = \frac{\sigma_{13}}{\sqrt{1-d_1}\sqrt{1-d_3}}$$

for

$$\overline{\sigma}_{13} = \frac{1}{(F_{11}F_{22}F_{33})}[F_{11}]^{1/2}\sigma_{13}[F_{33}]^{1/2} = \overline{\sigma}_{31} = \frac{\sigma_{13}}{\sqrt{1-d_1}\sqrt{1-d_1}}$$

Page 1488 *Substitute Equation (6)*

$$\overline{\sigma} = M^{-1}(D)\sigma = \left(\sqrt{I-D} \otimes \sqrt{I-D}\right)^{-1} \sigma \qquad \overline{\varepsilon}_e = M(D)\varepsilon_e = \left(\sqrt{I-D} \otimes \sqrt{I-D}\right)\varepsilon_e$$

where $(A \otimes B)^{-1} C = A^{-1}CB^{-T}$ and $(A \otimes B)C = ACB^T$

for

$$\overline{\sigma} = M^{-1}(D)\sigma = \left(\sqrt{I-D}\varepsilon\sqrt{I-D}\right)^{-1} \sigma \qquad \overline{\varepsilon}_e = M(D)\varepsilon_e = \left(\sqrt{I-D}\varepsilon\sqrt{I-D}\right)\varepsilon_e$$

On page 1490: *Equation (17) substitute*

$$“\dot{\lambda}^p = \left\langle \begin{array}{ll} \frac{1}{L} < A'\dot{\varepsilon} >, & g^p = 0 \\ 0, & g^p < 0 \end{array} \right. , \dot{\lambda}^d = \left\langle \begin{array}{ll} \frac{1}{L} < B'\dot{\varepsilon} >, & g^d = 0 \\ 0, & g^d < 0 \end{array} \right. ”$$

for

$$“\dot{\lambda}^p = \left\langle \begin{array}{ll} \frac{1}{L} < A\dot{\varepsilon} >, & g^p = 0 \\ 0, & g^p < 0 \end{array} \right. , \dot{\lambda}^d = \left\langle \begin{array}{ll} \frac{1}{L} < B\dot{\varepsilon} >, & g^d = 0 \\ 0, & g^d < 0 \end{array} \right. ”$$

Page 1491 *Substitute Equation (19).1*

$$\dot{\lambda}^d = \left\langle \frac{\left\{ [-\frac{\partial g^p}{\partial \bar{\sigma}} M^{-1} \frac{\partial \sigma}{\partial \varepsilon^p} M^{-1} \frac{\partial g^p}{\partial \bar{\sigma}} + \frac{\partial g^p}{\partial R} \frac{\partial R}{\partial p} \frac{\partial g^p}{\partial R}] \left[\frac{\partial g^d}{\partial Y} \frac{\partial Y}{\partial \varepsilon} \right] \dot{\varepsilon} + \left[\frac{\partial g^d}{\partial Y} \frac{\partial Y}{\partial \varepsilon^p} M^{-1} \frac{\partial g^p}{\partial \bar{\sigma}} \right] \left[\frac{\partial g^p}{\partial \bar{\sigma}} M^{-1} \frac{\partial \sigma}{\partial \varepsilon} \right] \dot{\varepsilon} \right\}}{\left\{ [\frac{\partial g^d}{\partial Y} \frac{\partial Y}{\partial D} \frac{\partial f^d}{\partial D} + \frac{\partial g^d}{\partial \gamma} \frac{\partial \gamma}{\partial \delta} \frac{\partial f^d}{\partial \gamma}][\frac{\partial g^p}{\partial \bar{\sigma}} M^{-1} \frac{\partial \sigma}{\partial \varepsilon^p} M^{-1} \frac{\partial g^p}{\partial \bar{\sigma}} + \frac{\partial g^p}{\partial R} \frac{\partial R}{\partial p} \frac{\partial g^p}{\partial R}] - \left[\frac{\partial g^p}{\partial \bar{\sigma}} \frac{\partial}{\partial D} [M^{-1}\sigma] \frac{\partial f^d}{\partial D} \right] \left[\frac{\partial g^d}{\partial Y} \frac{\partial Y}{\partial \varepsilon^p} M^{-1} \frac{\partial g^p}{\partial \bar{\sigma}} \right] \right\}} \right\rangle$$

for

$$\dot{\lambda}^d = \left\langle \frac{\left\{ [\frac{\partial g^p}{\partial \bar{\sigma}} M^{-1} \frac{\partial \sigma}{\partial \varepsilon^p} M^{-1} \frac{\partial g^p}{\partial \bar{\sigma}} + \frac{\partial g^p}{\partial R} \frac{\partial R}{\partial p} \frac{\partial g^p}{\partial R}] \left[\frac{\partial g^d}{\partial Y} \frac{\partial Y}{\partial \varepsilon} \right] \dot{\varepsilon} + \left[\frac{\partial g^d}{\partial Y} \frac{\partial Y}{\partial \varepsilon^p} M^{-1} \frac{\partial g^p}{\partial \bar{\sigma}} \right] \left[\frac{\partial g^p}{\partial \bar{\sigma}} M^{-1} \frac{\partial \sigma}{\partial \varepsilon} \right] \dot{\varepsilon} \right\}}{\left\{ [\frac{\partial g^d}{\partial Y} \frac{\partial Y}{\partial D} \frac{\partial f^d}{\partial D} + \frac{\partial g^d}{\partial \gamma} \frac{\partial \gamma}{\partial \delta} \frac{\partial f^d}{\partial \gamma}][\frac{\partial g^p}{\partial \bar{\sigma}} M^{-1} \frac{\partial \sigma}{\partial \varepsilon^p} M^{-1} \frac{\partial g^p}{\partial \bar{\sigma}} + \frac{\partial g^p}{\partial R} \frac{\partial R}{\partial p} \frac{\partial g^p}{\partial R}] - \left[\frac{\partial g^p}{\partial \bar{\sigma}} \frac{\partial}{\partial D} [M^{-1}\sigma] \frac{\partial f^d}{\partial D} \right] \left[\frac{\partial g^d}{\partial Y} \frac{\partial Y}{\partial \varepsilon^p} M^{-1} \frac{\partial g^p}{\partial \bar{\sigma}} \right] \right\}} \right\rangle$$

On page 1491: *Equation (20) substitute*

$$“\begin{aligned} A' &= -[\frac{\partial g^d}{\partial Y} \frac{\partial Y}{\partial D} \frac{\partial f^d}{\partial D} + \frac{\partial g^d}{\partial \gamma} \frac{\partial \gamma}{\partial \delta} \frac{\partial f^d}{\partial \gamma}] \left[\frac{\partial g^p}{\partial \bar{\sigma}} M^{-1} \frac{\partial \sigma}{\partial \varepsilon} \right] + [\frac{\partial g^p}{\partial \bar{\sigma}} \frac{\partial}{\partial D} [M^{-1}\sigma] \frac{\partial f^d}{\partial D}] \left[\frac{\partial g^d}{\partial Y} \frac{\partial Y}{\partial \varepsilon} \right] \\ B' &= -[\frac{\partial g^p}{\partial \bar{\sigma}} M^{-1} \frac{\partial \sigma}{\partial \varepsilon^p} M^{-1} \frac{\partial g^p}{\partial \bar{\sigma}} + \frac{\partial g^p}{\partial R} \frac{\partial R}{\partial p} \frac{\partial g^p}{\partial R}] \left[\frac{\partial g^d}{\partial Y} \frac{\partial Y}{\partial \varepsilon} \right] + \left[\frac{\partial g^d}{\partial Y} \frac{\partial Y}{\partial \varepsilon^p} M^{-1} \frac{\partial g^p}{\partial \bar{\sigma}} \right] \left[\frac{\partial g^p}{\partial \bar{\sigma}} M^{-1} \frac{\partial \sigma}{\partial \varepsilon} \right] \end{aligned}”$$

for

$$“\begin{aligned} A &= -[\frac{\partial g^d}{\partial Y} \frac{\partial Y}{\partial D} \frac{\partial f^d}{\partial D} + \frac{\partial g^d}{\partial \gamma} \frac{\partial \gamma}{\partial \delta} \frac{\partial f^d}{\partial \gamma}] \left[\frac{\partial g^p}{\partial \bar{\sigma}} M^{-1} \frac{\partial \sigma}{\partial \varepsilon} \right] + [\frac{\partial g^p}{\partial \bar{\sigma}} \frac{\partial}{\partial D} [M^{-1}\sigma] \frac{\partial f^d}{\partial D}] \left[\frac{\partial g^d}{\partial Y} \frac{\partial Y}{\partial \varepsilon} \right] \\ B &= -[\frac{\partial g^p}{\partial \bar{\sigma}} M^{-1} \frac{\partial \sigma}{\partial \varepsilon^p} M^{-1} \frac{\partial g^p}{\partial \bar{\sigma}} + \frac{\partial g^p}{\partial R} \frac{\partial R}{\partial p} \frac{\partial g^p}{\partial R}] \left[\frac{\partial g^d}{\partial Y} \frac{\partial Y}{\partial \varepsilon} \right] + \left[\frac{\partial g^d}{\partial Y} \frac{\partial Y}{\partial \varepsilon^p} M^{-1} \frac{\partial g^p}{\partial \bar{\sigma}} \right] \left[\frac{\partial g^p}{\partial \bar{\sigma}} M^{-1} \frac{\partial \sigma}{\partial \varepsilon} \right] \end{aligned}”$$

Page 1491 *Substitute Equation (22)*

$$\text{``}\dot{\sigma} = \frac{\partial \sigma}{\partial \varepsilon}\dot{\varepsilon} + \frac{\partial \sigma}{\partial \varepsilon^p} M \frac{1}{L} A\dot{\varepsilon} + \frac{\partial \sigma}{\partial D}\frac{1}{L} B\dot{\varepsilon} = E^{epd}\ \dot{\varepsilon} \qquad \dot{\varepsilon}^p, \dot{D} \geq 0$$

where $A = A' \dfrac{\partial g^p}{\partial \overline{\sigma}}$ and $B = B' \dfrac{\partial f^d}{\partial Y}$"

for

$$\text{``}\dot{\sigma} = \frac{\partial \sigma}{\partial \varepsilon}\dot{\varepsilon} + \frac{\partial \sigma}{\partial \varepsilon^p}\frac{1}{L} A\dot{\varepsilon} + \frac{\partial \sigma}{\partial D}\frac{1}{L} B\dot{\varepsilon} = E^{epd}\ \dot{\varepsilon} \qquad \dot{D} \geq 0\text{''}$$

Page 1496 *Substitute Equation (38)*

$$\sigma_{23} = F_4,\ \sigma_{11} = \sigma_{22} = \sigma_{12} = \sigma_{13} = 0$$

$$\text{``}\sqrt{\frac{J_{22}}{\Omega_{2s}^4} + \frac{J_{33}}{\Omega_{3s}^4}\ \frac{\overline{C_{44}}}{\Omega_{2s}^2 \Omega_{3s}^2}} F_4^2 + \sqrt{\left|\frac{H_2}{\Omega_{2s}^2} + \frac{H_3}{\Omega_{3s}^2}\right| \frac{\overline{C_{44}}}{\Omega_{2s}^2 \Omega_{3s}^2}} F_4 = \left(\gamma^* + \gamma_0\right) = 1\text{''}$$

for

$$\sigma_{23} \neq F_4,\ \sigma_{11} = \sigma_{22} = \sigma_{12} = \sigma_{13} = 0$$

$$\text{``}\sqrt{\frac{J_{22}}{\Omega_{2s}^4} + \frac{J_{33}}{\Omega_{3s}^4}\ \frac{2\overline{C_{44}}}{\Omega_{2s}^2 \Omega_{3s}^2}} F_4^2 + \sqrt{\left|\frac{H_2}{\Omega_{2s}^2} + \frac{H_3}{\Omega_{3s}^2}\right| \frac{2\overline{C_{44}}}{\Omega_{2s}^2 \Omega_{3s}^2}} F_4 = \left(\gamma^* + \gamma_0\right) = 1\text{''}$$

Page 1496 *Substitute Equation (39)*

$$\sigma_{13} = F_5,\ \sigma_{11} = \sigma_{22} = \sigma_{12} = \sigma_{23} = 0$$

$$\text{``}\sqrt{\frac{J_{11}}{\Omega_{1s}^4} + \frac{J_{33}}{\Omega_{3s}^4}\ \frac{\overline{C_{55}}}{\Omega_{1s}^2 \Omega_{3s}^2}} F_5^2 + \sqrt{\left|\frac{H_1}{\Omega_{1s}^2} + \frac{H_3}{\Omega_{3s}^2}\right| \frac{\overline{C_{55}}}{\Omega_{1s}^2 \Omega_{3s}^2}} F_5 = \left(\gamma^* + \gamma_0\right) = 1\text{''}$$

for

$$\sigma_{13} \neq F_5,\ \sigma_{11} = \sigma_{22} = \sigma_{12} = \sigma_{23} = 0$$

$$\text{``}\sqrt{\frac{J_{11}}{\Omega_{1s}^4} + \frac{J_{33}}{\Omega_{3s}^4}\ \frac{2\overline{C_{55}}}{\Omega_{1s}^2 \Omega_{3s}^2}} F_5^2 + \sqrt{\left|\frac{H_1}{\Omega_{1s}^2} + \frac{H_3}{\Omega_{3s}^2}\right| \frac{2\overline{C_{55}}}{\Omega_{1s}^2 \Omega_{3s}^2}} F_5 = \left(\gamma^* + \gamma_0\right) = 1\text{''}$$

Page 1496 *Substitute Equation (42)*

"Introducing the auxiliary parameters k_S^i (with i=23,13) defined as

$$\begin{aligned} k_S^{23} &= \left(\Omega_{2s}^2 \Omega_{3s}^2\right) = G_{23}^* / \overline{G_{23}} \\ k_S^{13} &= \left(\Omega_{1s}^2 \Omega_{3s}^2\right) = G_{13}^* / \overline{G_{13}} \end{aligned}\text{''}$$

for

"Introducing the auxiliary parameters k_i^S defined as

$$\begin{aligned} \left(k_{23}^S\right)^2 &= \left(\Omega_{2s}^2 \Omega_{3s}^2\right) = G_{23}^* / \overline{G_{23}} \\ \left(k_{13}^S\right)^2 &= \left(\Omega_{1s}^2 \Omega_{3s}^2\right) = G_{13}^* / \overline{G_{13}} \end{aligned}\text{''}$$

Page 1497 *Substitute Equation (43)*

“ $$\sqrt{\frac{J_{22} r_S^{23}}{k_S^{23}} + \frac{J_{33}}{k_S^{23} r_S^{23}} \frac{\overline{C_{44}}}{k_S^{23}} F_4^2} = (\gamma + \gamma_0) = 1$$
$$\sqrt{\frac{J_{11} r_S^{23}}{k_S^{13}} + \frac{J_{33}}{k_S^{13} r_S^{13}} \frac{\overline{C_{55}}}{k_S^{13}} F_5^2} = (\gamma + \gamma_0) = 1$$ ”

for

“ $$\sqrt{\frac{J_{22} r_{23}^S}{k_{23}^S} + \frac{J_{33}}{k_{23}^S r_{23}^S} \frac{2\overline{C_{44}}}{k_{23}^S} F_4^2} = (\gamma + \gamma_0) = 1$$
$$\sqrt{\frac{J_{11} r_{13}^S}{k_{13}^S} + \frac{J_{33}}{k_{13}^S r_{13}^S} \frac{2\overline{C_{55}}}{k_{13}^S} F_5^2} = (\gamma + \gamma_0) = 1$$ ”

Interlaminar Damage Model for Polymer Matrix Composites

PAOLO LONETTI, RAFFAELE ZINNO AND FABRIZIO GRECO
Department of Structural Engineering
University of Calabria, Cosenza, Italy

EVER J. BARBERO*
Mechanical and Aerospace Engineering
West Virginia University, Morgantown, WV 26506-6106, USA

(Received March 26, 2003)

ABSTRACT: A constitutive model for fiber-reinforced composite materials with damage and unrecoverable deformation, which for the first time accounts for interlaminar damage, is presented. The formulation is based on Continuous Damage Mechanics coupled with Classical Plasticity Theory in a consistent thermodynamic framework using internal state variables. In-plane damage and novel formulation of interlaminar damage are included in order to describe the main failure modes of laminates structures. A novel implementation of the constitutive model into a finite element formulation incorporating geometric nonlinearity is presented. The model uses a small number of adjustable parameters, which are identified from available experimental data. Comparisons with experimental data for composite laminates under torsion loading are shown to validate the model for interlaminar damage. Coupled material and geometrical nonlinear analysis with simultaneous in-plane and interlaminar damage is demonstrated. The effect of warping on interlaminar damage is shown to be significant.

KEY WORDS: damage, polymer, composite, plasticity, identification, torsion, warping, interlaminar

INTRODUCTION

THE NONLINEAR RESPONSE of engineering materials can be described by irreversible thermodynamics, which accounts for energy dissipation due to micromechanical change in the microstructures. The behavior of fiber-reinforced polymer matrix composite material is dominated by the heterogeneity of the material. Therefore, prediction of

*Author to whom correspondence should be addressed. E-mail: ebarbero@wvu.edu

0021-9983/03/16 1485–20 $10.00/0 DOI: 10.1177/002199803034741
© 2003 Sage Publications

Erratum: Vol. 38 No 9 p. 799-800

damage states and inelastic processes (yield) under multiaxial loading is complex in nature. The main damage modes can be attributed to fiber breaks, matrix cracking, fiber/matrix debonding, and so on, all of which decrease the integrity of the material. In order to predict the inelastic behavior and the damage modes, several approaches have been developed [1–5]. Continuous Damage Mechanics considers a measure of damage microcracks and voids area, randomly distributed in a representative volume element (RVE), affecting the material by a reduction of the material stiffness. The damage formulation introduced in [6] for in-plane damage, is extended here for interlaminar damage considering the general 3-D behavior of a composite laminate. The damage surface and the potential function are generalized in order to compute the interlaminar quantities. A new procedure is developed for model identification; namely to identify the through-the-thickness damage domain coefficients H_3 and J_{33} using interlaminar shear strength data F_4 and F_5. Furthermore, the 3D damage/plasticity model is complemented with geometrical nonlinearity in order to simulate the experimentally observed behavior under large rotations and deflections.

The model is defined by a coupled elasto-plastic/damage formulation, which accounts for stiffness reduction and unrecoverable deformations (yield). The formulation makes the use of the effective configuration and a second order damage tensor. Damage and unrecoverable deformation domains are expressed in the thermodynamic force space and in the effective stress, respectively. A return-mapping algorithm scheme is generalized in order to integrate the rate equations for both damage and unrecoverable deformation [7]. Computations are performed in conjunction with a finite element formulation, which accounts for damage, unrecoverable deformation, and geometric non-linearity.

Predictions of in-plane damage only were already validated for different laminates in [6,23,24]. In order to validate the model for interlaminar damage effects, comparison with experimental data [8] under torque loading are presented. The analysis is performed for coupled material and geometry nonlinearities, by using a corotational approach. The interlaminar effects are highlighted in order to show the differences between the in-plane and interlaminar damage contributions.

THEORETICAL FORMULATION

A continuum damage mechanics model for an orthotropic lamina, accounting for interlaminar effects, is derived in this section and assembled into a laminate model. A second order damage tensor D is used to represent damage following Kachanov–Rabotnov's approach [9,10]. Lamina experimental results evidence different damage modes and evolution for longitudinal, transverse, and shear loading [26]. In addition, shear loading leads to longitudinal and mostly transverse damage [27–29]. Therefore, it is assumed that damage is orthotropic and that the principal directions of damage are aligned with the material coordinates. Then, the second order damage tensor can be represented in the principal system, as

$$D_i = \sum_{i=1}^{3} d_i n_i \otimes n_i \tag{1}$$

where $\otimes$ denotes the dyad product of tensors [25], n_i are the orthogonal principal directions, which in the proposed model coincide with the fiber, matrix, and thickness directions, d_i are the eigenvalues of the D tensor, which represents the damaged area ratio along the n_i directions. The dual variable of the damage tensor is the integrity tensor Ω which represents the undamaged area ratio. By the spectral decomposition theorem [11], the integrity tensor in the principal direction assumes the following form

$$\Omega_i = \sum_{i=1}^{n} \overline{\omega_i}(n_i \otimes n_i) \tag{2}$$

The use of damage and integrity tensors describes a mapping between the effective and damaged configurations by a linear operator f, as $f : c \to \bar{c}$. By the square root theorem [11], a unique transformation connects the damage and integrity tensor $\Omega = \sqrt{I - D}$. The integrity tensor is always symmetric and positive, because the net area reduction must be positive definite during damage evolution [2].

In order to have a symmetric effective stress tensor, avoiding formulating the constitutive model as Cosserat or micropolar continua, a symmetrization technique is used [12,13]. Using Nanson's formula [12], which relates the current and the effective surface area in a symmetrization form, it is possible to derive the relationship between the effective stress and the actual stress tensor by equilibrium equivalence as

$$\bar{\sigma} = J^{-1}\left[F^{(1/2)}\right]^T \sigma \left[F^{(1/2)}\right] \tag{3}$$

where J is the Jacobian and the tensor F relates the current damaged configuration and the corresponding fictitious undamaged one. In this way, the effective stress components assume the following expressions

$$\begin{aligned}
\bar{\sigma}_{11} &= \frac{1}{(F_{11}F_{22}F_{33})} F_{11}\sigma_{11} = \frac{\sigma_{11}}{(1-d_1)} \\
\bar{\sigma}_{22} &= \frac{1}{(F_{11}F_{22}F_{33})} F_{22}\sigma_{22} = \frac{\sigma_{22}}{(1-d_2)} \\
\bar{\sigma}_{33} &= \frac{1}{(F_{11}F_{22}F_{33})} F_{33}\sigma_{33} = \frac{\sigma_{33}}{(1-d_3)} \\
\bar{\sigma}_{12} &= \frac{1}{(F_{11}F_{22}F_{33})} [F_{11}]^{1/2}\sigma_{12}[F_{22}]^{1/2} = \bar{\sigma}_{21} = \frac{\sigma_{12}}{\sqrt{1-d_1}\sqrt{1-d_2}} \\
\bar{\sigma}_{13} &= \frac{1}{(F_{11}F_{22}F_{33})} [F_{11}]^{1/2}\sigma_{13}[F_{33}]^{1/2} = \bar{\sigma}_{31} = \frac{\sigma_{13}}{\sqrt{1-d_1}\sqrt{1-d_3}} \\
\bar{\sigma}_{23} &= \frac{1}{(F_{11}F_{22}F_{33})} [F_{22}]^{1/2}\sigma_{23}[F_{33}]^{1/2} = \bar{\sigma}_{32} = \frac{\sigma_{32}}{\sqrt{1-d_2}\sqrt{1-d_3}}
\end{aligned} \tag{4}$$

while, in the principal reference system, the diagonal components of the tensor F reduces to

$$F_{11} = \sqrt{\frac{(1-d_2)(1-d_3)}{(1-d_1)}} \quad F_{22} = \sqrt{\frac{(1-d_1)(1-d_3)}{(1-d_2)}} \quad F_{33} = \sqrt{\frac{(1-d_1)(1-d_2)}{(1-d_3)}} \tag{5}$$

In this way, by Equations (1)–(5), a fourth order tensor M, called effective damage tensor, can be introduced, in order to define a linear operator, which relates the stress and the strain in the actual and damaged configurations respectively, in the following form [13]

$$\bar{\sigma} = M^{-1}(D)\sigma = \left(\sqrt{I-D}\overset{\otimes}{\cdot}\sqrt{I-D}\right)^{-1}\sigma \quad \bar{\varepsilon}_e = M(D)\varepsilon_e = \left(\sqrt{I-D}\overset{\otimes}{\cdot}\sqrt{I-D}\right)\varepsilon_e \tag{6}$$

where $(A \otimes B)^{-1}C = A^{-1}CB^T$ & $(A \otimes B)C = ACB^T$

By the energy equivalence hypothesis [12–14], it is possible to define Hooke's law in the effective $\bar{c}$ and damaged c configuration as

$$\bar{\sigma} = \overline{E_e}(D)\bar{\varepsilon}_e \qquad \sigma = E_e(D)\varepsilon_e \tag{7}$$

where an over-bar indicates that the quantity is evaluated in the effective configuration and the subscript e denotes quantities in the elastic domain.

The constitutive equations are derived by thermodynamic principles and complementary laws. The expression of the Helmholtz function given in [6] assumes an additive decomposition into stored elastic energy terms and additional terms related to the evolution of the internal parameters. In order to satisfy the Clausius–Duhem inequality the following thermodynamic state laws can be obtained

$$\begin{aligned} &\sigma = E(D)(\varepsilon - \varepsilon^p) \\ &Y = \frac{1}{2}(\varepsilon - \varepsilon^p)\frac{\partial E(D)}{\partial D}(\varepsilon - \varepsilon^p) \end{aligned} \tag{8}$$

complemented by the evolution equations assumed in [6] as follows

$$\begin{aligned} &R = -c_1^p p \\ &\gamma = c_1^d[\exp(\delta/c_2^d) - 1] \end{aligned} \tag{9}$$

where $\psi(\varepsilon, D, p, \delta)$ is the Helmholtz free energy and (σ, Y, R, γ) are the thermodynamic forces associated to the internal state variables $(\varepsilon D, p, \delta)$. It is worth noting that in this paper the second order tensor Y includes the Y_{33} component, which represents the energy release rate for the interlaminar shear damage.

The evolution of the internal variables can be defined by using the Legendre–Fenchel transformation of the dissipation potential, the principle of maximum entropy, and

Lagrange minimization method [15], by which the following expressions describe the development of the inelastic effects

$$\begin{aligned} &\dot{\bar{\varepsilon}}^p = \dot{\lambda}^p\frac{\partial g^p}{\partial \bar{\sigma}} \quad ; \quad \dot{p} = \dot{\lambda}^p\frac{\partial g^p}{\partial R} \\ &\dot{D} = \dot{\lambda}^d\frac{\partial f^d}{\partial Y} \quad ; \quad \dot{\delta} = \dot{\lambda}^d\frac{\partial f^d}{\partial \gamma} \end{aligned} \tag{10}$$

where $\dot{\lambda}^d$, $\dot{\lambda}^p$ are the damage and unrecoverable-deformation multipliers respectively. The unrecoverable-deformation (yield) domain g^p and damage-potential function f^d are defined in the next section.

DAMAGE AND UNRECOVERABLE DEFORMATION

An anisotropic damage criterion expressed in tensorial form, introducing fourth and second order tensors, J and H is used as in [6]. It defines a multiaxial limit surface in the thermodynamic force space Y that bounds the damage domain. The damage evolution is defined by a damage potential nonassociate to the damage surface and by an isotropic hardening law. The damage surface is

$$g^d = \left(Y_{ij} \cdot J_{ijhk} Y_{hk}\right)^{1/2} + \left(\left|H_{ij} \cdot Y_{ij}\right|\right)^{1/2} - \gamma(\delta) - \gamma_0 \tag{11}$$

and the potential function is

$$f^d = \left(Y_{ij} \cdot J_{ijhk} Y_{hk}\right)^{1/2} - \gamma(\delta) - \gamma_0 \tag{12}$$

where

$$\gamma(\delta) = c_1^d\left[\exp(\delta/c_2^d) - 1\right] \tag{13}$$

The J and H tensors are determined by available data on a single composite lamina, while the adjustable parameters c_1^d and c_2^d are determined by using the experimental in-plane shear strength–strain data.

Unrecoverable-deformation (yield) evolution is modeled by classical plasticity formulation [16]. An associate flow rule is assumed in the effective stress space, coupling plasticity and damage effects. The unrecoverable-deformation surface is a function of the thermodynamic forces in the effective configuration $(\bar{\sigma}, R)$. Therefore, the unrecoverable-deformation (yield) surface, which accounts for interlaminar terms, is

$$g^p = f_{ij}\bar{\sigma}_i\bar{\sigma}_j + f_i\bar{\sigma}_i - (R(p) + R_0); \tag{14}$$

where $(i = 1, 2 \ldots 6)$, R_0 is the unrecoverable-deformation energy threshold. A Tsai–Wu criterion shape is chosen for Equation (14) because of its ability to represent different behavior among the different load paths in stress space. The coefficients f_i assume the following form

$$
\begin{aligned}
&f_1=\frac{1}{F_{1t}}-\frac{1}{F_{1c}};\quad f_2=\frac{1}{F_{2t}}-\frac{1}{F_{2c}};\quad f_{11}=\frac{1}{F_{1t}F_{1c}};\quad f_{22}=\frac{1}{F_{2t}F_{2c}};\\
&f_{44}=\frac{1}{F_4^2};\quad f_{55}=\frac{1}{F_5^2};\quad f_{66}=\frac{1}{F_6^2};\quad f_{12}\cong-\frac{0.5}{(F_{1t}F_{1c}F_{2t}F_{2c})^{1/2}}
\end{aligned}
\tag{15}
$$

The parameters F_i are the strength values in tension, compression, in-plane, and out-of-plane shear for a single composite lamina. These values are tabulated in literature, or they can be easily obtained following standardized test methods [18–20].

CONSTITUTIVE EQUATIONS

The incremental stress–strain relations for damage and unrecoverable deformation evolution can be obtained from Equation (10). By using the additive decomposition hypothesis [21], which splits the total strain rate into elastic and plastic contributions, the rate stress assumes the following expression

$$
\dot{\sigma}=\frac{\partial\sigma}{\partial\varepsilon}\dot{\varepsilon}+\frac{\partial\sigma}{\partial\varepsilon^p}\dot{\varepsilon}^p+\frac{\partial\sigma}{\partial D}\dot{D}
\tag{16}
$$

The evolution equations can be obtained by the flow Equations (10), where damage and unrecoverable deformation multipliers are expressed as

$$
\begin{aligned}
&\dot{\lambda}^p=\begin{cases}\dfrac{1}{L}<A\dot{\varepsilon}>, & g^p=0\\ 0, & g^p<0\end{cases}\\
&\dot{\lambda}^d=\begin{cases}\dfrac{1}{L}<B\dot{\varepsilon}>, & g^d=0\\ 0, & g^d<0\end{cases}
\end{aligned}
\tag{17}
$$

where <.. > denote the positive part, L is a scalar and A, B represent fourth order non-linear operators, which relate the evolution of inelastic effects to the total deformation rate. In order to characterize the A and B tensors, the consistency condition ($\dot{g}^d=g^d=0;\dot{g}^p=g^p=0$), for both plasticity and damage must be used, leading to the following system of nonlinear equations

$$
\begin{aligned}
&\dot{g}^d=\frac{\partial g^d}{\partial Y}\dot{Y}+\frac{\partial g^d}{\partial\gamma}\dot{\gamma}=0 \qquad g^d=0\\
&\dot{g}^p=\frac{\partial g^p}{\partial\overline{\sigma}}\dot{\overline{\sigma}}+\frac{\partial g^p}{\partial R}\dot{R}=0 \qquad g^p=0
\end{aligned}
\tag{18}
$$

Introducing Equation (8)–(9) into Equation (18) and solving for the scalar parameters $\dot{\lambda}^d$ and $\dot{\lambda}^p$we obtain

$$
\begin{aligned}
\dot{\lambda}^d=\;&\\
&\left\langle\left\{\left[\frac{\partial g^p}{\partial\overline{\sigma}}M^{-1}\frac{\partial\sigma}{\partial\varepsilon^p}M^{-1}\frac{\partial g^p}{\partial\overline{\sigma}}+\frac{\partial g^p}{\partial R}\frac{\partial R}{\partial p}\frac{\partial g^p}{\partial R}\right]\left[\frac{\partial g^d}{\partial Y}\frac{\partial Y}{\partial\varepsilon}\right]\dot{\varepsilon}+\left[\frac{\partial g^d}{\partial Y}\frac{\partial Y}{\partial\varepsilon^p}M^{-1}\frac{\partial g^p}{\partial\overline{\sigma}}\right]\left[\frac{\partial g^p}{\partial\overline{\sigma}}M^{-1}\frac{\partial\sigma}{\partial\varepsilon}\right]\dot{\varepsilon}\right\}\Big/\right.\\
&\quad\left\{\left[\frac{\partial g^d}{\partial Y}\frac{\partial Y}{\partial D}\frac{\partial f^d}{\partial D}+\frac{\partial g^d}{\partial\gamma}\frac{\partial\gamma}{\partial\delta}\frac{\partial f^d}{\partial\gamma}\right]\left[\frac{\partial g^p}{\partial\overline{\sigma}}M^{-1}\frac{\partial\sigma}{\partial\varepsilon^p}M^{-1}\frac{\partial g^p}{\partial\overline{\sigma}}+\frac{\partial g^p}{\partial R}\frac{\partial R}{\partial p}\frac{\partial g^p}{\partial R}\right]\right.\\
&\quad\left.\left.-\left[\frac{\partial g^p}{\partial\overline{\sigma}}\frac{\partial}{\partial D}[M^{-1}\sigma]\frac{\partial f^d}{\partial D}\right]\left[\frac{\partial g^d}{\partial Y}\frac{\partial Y}{\partial\varepsilon^p}M^{-1}\frac{\partial g^p}{\partial\overline{\sigma}}\right]\right\}\right\rangle\\
\dot{\lambda}^p=\;&\\
&\left\langle\left\{-\left[\frac{\partial g^d}{\partial Y}\frac{\partial Y}{\partial D}\frac{\partial f^d}{\partial D}+\frac{\partial g^d}{\partial\gamma}\frac{\partial\gamma}{\partial\delta}\frac{\partial f^d}{\partial\gamma}\right]\left[\frac{\partial g^p}{\partial\overline{\sigma}}M^{-1}\frac{\partial\sigma}{\partial\varepsilon}\right]\dot{\varepsilon}+\left[\frac{\partial g^p}{\partial\overline{\sigma}}\frac{\partial}{\partial D}[M^{-1}\sigma]\frac{\partial f^d}{\partial D}\right]\left[\frac{\partial g^d}{\partial Y}\frac{\partial Y}{\partial\varepsilon}\right]\dot{\varepsilon}\right\}\Big/\right.\\
&\quad\left\{\left[\frac{\partial g^d}{\partial Y}\frac{\partial Y}{\partial D}\frac{\partial f^d}{\partial D}+\frac{\partial g^d}{\partial\gamma}\frac{\partial\gamma}{\partial\delta}\frac{\partial f^d}{\partial\gamma}\right]\left[\frac{\partial g^p}{\partial\overline{\sigma}}M^{-1}\frac{\partial\sigma}{\partial\varepsilon^p}M^{-1}\frac{\partial g^p}{\partial\overline{\sigma}}+\frac{\partial g^p}{\partial R}\frac{\partial R}{\partial p}\frac{\partial g^p}{\partial R}\right]\right.\\
&\quad\left.\left.-\left[\frac{\partial g^p}{\partial\overline{\sigma}}\frac{\partial}{\partial D}[M^{-1}\sigma]\frac{\partial f^d}{\partial D}\right]\left[\frac{\partial g^d}{\partial Y}\frac{\partial Y}{\partial\varepsilon^p}M^{-1}\frac{\partial g^p}{\partial\overline{\sigma}}\right]\right\}\right\rangle
\end{aligned}
\tag{19}
$$

Introducing the Equations (19) in Equations (17) the A and B tensors can be uniquely determined as

$$
\begin{aligned}
A&=-\left[\frac{\partial g^d}{\partial Y}\frac{\partial Y}{\partial D}\frac{\partial f^d}{\partial D}+\frac{\partial g^d}{\partial\gamma}\frac{\partial\gamma}{\partial\delta}\frac{\partial f^d}{\partial\gamma}\right]\left[\frac{\partial g^p}{\partial\overline{\sigma}}M^{-1}\frac{\partial\sigma}{\partial\varepsilon}\right]+\left[\frac{\partial g^p}{\partial\overline{\sigma}}\frac{\partial}{\partial D}[M^{-1}\sigma]\frac{\partial f^d}{\partial D}\right]\left[\frac{\partial g^d}{\partial Y}\frac{\partial Y}{\partial\varepsilon}\right]\\
B&=\left[\frac{\partial g^p}{\partial\overline{\sigma}}M^{-1}\frac{\partial\sigma}{\partial\varepsilon^p}M^{-1}\frac{\partial g^p}{\partial\overline{\sigma}}+\frac{\partial g^p}{\partial R}\frac{\partial R}{\partial p}\frac{\partial g^p}{\partial R}\right]\left[\frac{\partial g^d}{\partial Y}\frac{\partial Y}{\partial\varepsilon}\right]+\left[\frac{\partial g^d}{\partial Y}\frac{\partial Y}{\partial\varepsilon^p}M^{-1}\frac{\partial g^p}{\partial\overline{\sigma}}\right]\left[\frac{\partial g^p}{\partial\overline{\sigma}}M^{-1}\frac{\partial\sigma}{\partial\varepsilon}\right]
\end{aligned}
\tag{20}
$$

It is worth noting that Equation (16) can be expressed symbolically in the form

$$
\dot{\sigma}=E^{\mathrm{epd}}\dot{\varepsilon}
\tag{21}
$$

where $E^{\mathrm{epd}}$is a nonlinear operator, since it depends on the direction of $\dot{\varepsilon}$ and the current state represented by thermodynamic forces (Y,σ,γ,R) or by the kinematic variables $(D,\varepsilon^p,\delta,p)$. The nonlinear problem is solved by a return-mapping algorithm [17]. In particular, using an incremental form, $\Delta\lambda^d$ and $\Delta\lambda^p$ are defined so that the state defined by $(Y+\Delta Y,\sigma+\Delta\sigma,\gamma+\Delta\gamma,R+\Delta R)$ lies in the damage and unrecoverable deformation surfaces, at least in a first approximation. The elasto-plastic damaged stiffness, at the current increment, can be determined directly by the use of Equation (16),(17) as

$$\dot{\sigma} = \frac{\partial \sigma}{\partial \varepsilon}\dot{\varepsilon} + \frac{\partial \sigma}{\partial \varepsilon^p}\frac{1}{L}A\dot{\varepsilon} + \frac{\partial \sigma}{\partial D}\frac{1}{L}B\dot{\varepsilon} = E^{epd}\dot{\varepsilon}, \quad \dot{\varepsilon}^p, \dot{D} \geq 0 \tag{22}$$

where $A = A' \partial g^p/\partial \sigma$ & $B = B' \partial f^d/\partial Y$

$$E^{epd} = \left[E(D)\left(1 - \frac{1}{L}A\right) + \frac{\partial \sigma}{\partial D}\frac{1}{L}B\right] \tag{23}$$

While the first two terms in Equation (22) are the classical terms for plasticity, the third term describes the stiffness reduction due to an increment of damage.

FINITE ELEMENT FORMULATION

A displacement-based finite element formulation is used. The body of a laminate is represented by a series of layers with different thickness and orientations. Two reference systems, global (x_i, $i=1..3$) and material (e_1, $i=1..3$) are used. The local reference axis e_1 is aligned with the fibers direction, e_3 points through the thickness of the laminate, and e_2 lays on the midsurface of the layer and is perpendicular to e_1 and e_3 ($e_2 = e_3 \times e_1$).

The geometry is discretized by three-dimensional composite elements. The material non-linearity is tracked at each integration point, for which damage and unrecoverable deformation are recovered. An isoparametric formulation is adopted. The displacement field varies linearly over the thickness and quadratically in the plane of the element. The quadratic element has 16 nodes. In order to reduce computational costs related to conventional solid element, a single three-dimensional element includes several laminae by adopting a number of integration points depending on the lay-up and thickness of layers. The computations were performed by inserting the proposed material model into the FE code LUSAS^{TM}.

Considering a body B, in which the internal stresses σ, the distributed load q, and the concentrated loads f constitute an equilibrated system, applying an arbitrary virtual displacement pattern δu^* compatible with the internal strain $\delta\varepsilon^*$, the principle of virtual displacement can be written as

$$\int_V \delta\varepsilon^{*T}\sigma dV - \int_S \delta u^{*T} q dS - \sum_{i=1}^{n_f} \delta u_i^T f_i = 0 \tag{24}$$

where n_f is the number of the concentrated loads. Introducing the shape functions N and nodal displacement d and using the finite element discretization process, Equation (24) becomes

$$\delta d^T\left(\int_V B^T \sigma dV - \int_S N^T q dS - f\right) = 0, \tag{25}$$

where S is the area in the $x_1 - x_2$ plane, and $V = [S \ x \ t]$, with t total thickness of the laminate.

To predict the stiffness reduction and the increment of unrecoverable-deformations, an incremental step-by-step analysis is adopted [22]. For an increment of load, Equation (25) becomes

$$\int_V B^T \Delta\sigma dV - \int_S N^T \Delta q dS - \sum_{i=1}^{n} \Delta f = 0 \tag{26}$$

where $\Delta\sigma$ represents the stress tensor increment for damage and unrecoverable-deformation evolution. The constitutive relation can be taken in the form of Equation (21), for which the tangent stiffness at each integration point level is defined by the following expressions

$$E^{epd} = \begin{cases} \left[E(D)\left(1 - \frac{1}{L}A\right) + \frac{\partial \sigma}{\partial D}\frac{1}{L}B\right] & \dot{D}, \quad \dot{\varepsilon}^p \geq 0 \\ \left[E(D) + \frac{\partial \sigma}{\partial D}\frac{1}{L}B\right] & \dot{D} \geq 0, \quad \dot{\varepsilon}^p \leq 0 \\ \left[E(D)\left(1 - \frac{1}{L}A\right)\right] & \dot{D} \leq 0, \quad \dot{\varepsilon}^p \geq 0 \\ [E(D)]\dot{D}, \quad \dot{\varepsilon}^p \leq 0 & \dot{D} \leq 0, \quad \dot{\varepsilon}^p \leq 0 \end{cases} \tag{27}$$

Substituting Equation (27) into Equation (26), we get

$$[K_{epd}][\Delta \cancel{\psi}\, \underset{\sim}{u}] = [\Delta F] \tag{28}$$

where the stiffness matrix and the load vector are

$$[K_{epd}] = \int_V [B^T E^{epd} B] dV$$
$$[\Delta F] = \int_S N^T \Delta q dS + \Delta f \tag{29}$$

In order to describe the behavior of a laminate under torsion test, a nonlinear analysis is performed for both material and geometrical effects using a corotation approach. The strains are expressed with respect to a follower frame, which is fixed to the element and rotates with it in 3-D space. In this way, rotations (mainly emanating from rigid body motion) and stretches can be treated independently. The geometric nonlinearity is incorporated via the rotation of the local system. Small strains are assumed and engineering stress and strain measures are appropriate in this formulation. The formulation separates the rotations from the stretches using the polar decomposition theorem and it allows the use of linear elements within a corotational framework. The proposed damage and unrecoverable deformation evolution are incorporated into a finite element program (LUSAS) using an User Material Subroutine. The incremental form of the governing equation can be written as

$$[K^M_{NL} + K^G_{NL}][\Delta u] = \Delta F \tag{30}$$

where Δu is the incremental displacement, K^M_{NL} is the nonlinear material tangent stiffness matrix, K^G_{NL} is nonlinear geometrical contribution, and ΔF is out balance force.

NUMERICAL IMPLEMENTATION

Damage and unrecoverable-deformation are monitored at the Gauss integration points. In order to accurately integrate numerically the rate equations, an algorithm for coupled damage and unrecoverable-deformations is developed, as follows. First, compute the strain and stress increment $\Delta\varepsilon$, $\Delta\sigma$ in the local coordinate system for each lamina at each gauss point

$$[\Delta\varepsilon]_L = T_k[\Delta\varepsilon]_G; \quad [\Delta\sigma]_L = T_k[\Delta\sigma]_G \tag{31}$$

where the T_k is a coordinate matrix transformation [18]. Subscripts L, G, indicate local and global coordinates, respectively. An elastic predictor and inelastic corrector scheme is used to determine the effect of a small strain increment $\Delta\varepsilon$. In this way the initial increment is purely elastic. The damage and unrecoverable-deformations are evaluated in order to check if the inelastic effects grow. Four different conditions define all possible cases

$$g^d \geq 0 \quad g^p \geq 0 \quad \text{Damage and U.D. evolution} \tag{32}$$

$$g^d < 0 \quad g^p \geq 0 \quad \text{U.D. evolution} \tag{33}$$

$$g^d \geq 0 \quad g^p < 0 \quad \text{Damage evolution} \tag{34}$$

$$g^d < 0 \quad g^p < 0 \quad \text{Elastic behavior} \tag{35}$$

The evolution of the damage and unrecoverable-deformation variables is subjected to the return-mapping algorithm. In this way, the damage and unrecoverable-deformation domains are linearized to the first order as

$$\begin{aligned} g^d &\cong g^d_{i+1} + \left.\frac{\partial g^d}{\partial Y}\right|^k_{i+1}(Y - Y^k_{i+1}) + \left.\frac{\partial g^d}{\partial \gamma}\right|^k_{i+1}(\gamma - \gamma^k_{i+1}) \\ g^p &\cong g^p_{i+1} + \left.\frac{\partial g^p}{\partial \bar{\sigma}}\right|^k_{i+1}(\bar{\sigma} - \bar{\sigma}^k_{i+1}) + \left.\frac{\partial g^p}{\partial R}\right|^k_{i+1}(R - R^k_{i+1}) \end{aligned} \tag{36}$$

where the subscript $(i+1)$ indicates load step, while superscript (k) represent the iteration number. The thermodynamic forces (Y, γ, R) and the effective stress $\bar{\sigma}$, can be expressed

by using Equations (8),(9) in terms of the kinematic quantities (D,ε ε^p) and the damage and unrecoverable-deformation multipliers as

$$\begin{aligned}
&(Y^{k+1}_{i+1} - Y^k_{i+1}) = \left.\frac{\partial Y}{\partial D}\right|^k_{i+1}(D^{k+1}_{i+1} - D^k_{i+1}) + \left.\frac{\partial Y}{\partial \varepsilon}\right|^k_{i+1}(\varepsilon^{k+1}_{i+1} - \varepsilon^k_{i+1}) + \left.\frac{\partial Y}{\partial \varepsilon^p}\right|^k_{i+1}\left(\varepsilon^{p(k+1)}_{i+1} - \varepsilon^{p(k)}_{i+1}\right) \\
&(\gamma^{k+1}_{i+1} - \gamma^k_{i+1}) = \left.\frac{\partial \gamma}{\partial \delta}\right|^k_{i+1} - \Delta\lambda^d \\
&\left(\bar{\sigma}^{(k+1)}_{i+1} - \bar{\sigma}^{(k)}_{i+1}\right) = M^{-1}\left(\sigma^{(k+1)}_{i+1} - \sigma^{(k)}_{i+1}\right) \\
&(R^{k+1}_{i+1} - R^k_{i+1}) = \left.\frac{\partial R}{\partial p}\right|^k_{i+1} - \Delta\lambda^p \\
&\left(\sigma^{(k+1)}_{i+1} - \sigma^{(k)}_{i+1}\right) = \left[E(D)(\varepsilon^{k+1}_{i+1} - \varepsilon^k_{i+1}) + \left.\frac{\partial \sigma}{\partial \varepsilon^p}\right|^k_{i+1}\left(\varepsilon^{p(k+1)}_{i+1} - \varepsilon^{p(k)}_{i+1}\right) + \left.\frac{\partial \sigma}{\partial D}\right|^k_{i+1}(D^{k+1}_{i+1} - D^k_{i+1})\right] \\
&(D^{k+1}_{i+1} - D^k_{i+1}) = \Delta\lambda^d \left.\frac{\partial f^d}{\partial Y}\right|^k_{i+1}\left(\varepsilon^{p(k+1)}_{i+1} - \varepsilon^{p(k)}_{i+1}\right) = \Delta\lambda^p \left.\frac{\partial g^p}{\partial Y}\right|^k_{i+1}
\end{aligned} \tag{37}$$

In the general case when damage and unrecoverable-deformations grow, Equations (37) are functions $\Delta\lambda^d$ and $\Delta\lambda^p$ only, leading to linear system that can be solved easily. The last step is to check if the damage state variables D_i have reached the critical values D_i^{CR}. When a damage component exceeds the critical value, it signals the appearance of a macro-crack. Therefore, the damage component is set to nearly one $(D_i = 1)$ to enforce total reduction of stiffness at the Gauss point.

MODEL IDENTIFICATION

The model uses a number of internal parameters that are explicitly related to the experimental material properties. The damage domain is defined by a fourth and second order tensor J and H respectively, while damage evolution, which is assumed to be isotropic, is expressed by an exponential function depending of two constants c^d_1 and c^d_2. The idea is to compare the Tsai-Wu criteria with the damage domain in the effective stress space, obtaining a linear system, with solutions that characterize uniquely the J and H tensors. The in-plane coefficients J_{11}, J_{22}, H_1 and H_2 are directly related to in-plane material properties (E_1, E_2, G_{12}, F_{1t}, F_{1c}, F_{2t}, F_{2c}, F_6) through equations described in [6]. Interlaminar damage is represented by the coefficients J_{33} and H_3, and their relationship to available material properties is introduced next.

For an interlaminar stress state only, the damage surface g^d in thermodynamic-force space Y is given by Equation (11), which can be written explicitly in terms of stress by using Equation (8). In stress space, g^d has the shape of the Tsai–Wu failure surface. For the undamaged material $\gamma = 0$, and g^d is smaller than the Tsai–Wu surface. At failure $\gamma^* + \gamma = 1$, and g^d coincides in shape and magnitude with the Tsai–Wu surface. When only interlaminar stresses are present, g^d at failure reduces to

$$\sigma_{23} \neq F_4, \qquad \sigma_{11} = \sigma_{22} = \sigma_{12} = \sigma_{13} = 0$$

$$\sqrt{\frac{J_{22}}{\Omega_{2s}^4} + \frac{J_{33}}{\Omega_{3s}^4}\frac{2\overline{C_{44}}}{\Omega_{2s}^2\Omega_{3s}^2}}F_4^2 + \sqrt{\left|\frac{H_2}{\Omega_{2s}^2} + \frac{H_3}{\Omega_{3s}^2}\right|\frac{2\overline{C_{44}}}{\Omega_{2s}^2\Omega_{3s}^2}}F_4 = (\gamma^* + \gamma_0) = 1 \tag{38}$$

and

$$\sigma_{13} \neq F_5, \qquad \sigma_{11} = \sigma_{22} = \sigma_{12} = \sigma_{23} = 0$$

$$\sqrt{\frac{J_{11}}{\Omega_{1s}^4} + \frac{J_{33}}{\Omega_{3s}^4}\frac{2\overline{C_{55}}}{\Omega_{1s}^2\Omega_{3s}^2}}F_5^2 + \sqrt{\left|\frac{H_1}{\Omega_{1s}^2} + \frac{H_3}{\Omega_{3s}^2}\right|\frac{2\overline{C_{55}}}{\Omega_{1s}^2\Omega_{3s}^2}}F_5 = (\gamma^* + \gamma_0) = 1 \tag{39}$$

where $\Omega_{1s}, \Omega_{2s}, \Omega_{3s}$, are the critical values of integrity at interlaminar shear failure in the longitudinal, transverse, and thickness direction, respectively. Since the shear strength values are independent on the sign of the shear stress ($\sigma_4 = F_4$ or $\sigma_4 = -F_4$, and $\sigma_5 = F_5$ or $\sigma_5 = -F_5$), the linear terms of Equations (38), (39), must be zero, leading to the following conditions

$$\left|\frac{H_2}{\Omega_{2s}^2} + \frac{H_3}{\Omega_{3s}^2}\right| = 0 \quad \text{and} \quad \left|\frac{H_1}{\Omega_{1s}^2} + \frac{H_3}{\Omega_{3s}^2}\right| = 0 \tag{40}$$

Solving Equation (40) for H_2 and H_3 we obtain

$$H_2 = -\frac{\Omega_{2s}^2}{\Omega_{3s}^2}H_3 = -r_s^{23}H_3$$
$$H_3 = -\frac{\Omega_{3s}^2}{\Omega_{1s}^2}H_1 = -r_s^{13}H_1 \tag{41}$$

where the r_s^i variables, (with $i = 23{,}13$) represent the ratio between the integrity values along the transverse/thickness and thickness/fiber directions, respectively. From experimental observations, the value r_s^{13} is constrained to be less than 1, because of lower through-the-thickness strength than longitudinal (fiber) strength. Introducing the auxiliary parameters k_i^S defined as

$$(k_{23}^S) = (\Omega_{2s}^2\Omega_{3s}^2) = G_{23}^*/\overline{G_{23}}$$
$$(k_{13}^S) = (\Omega_{1s}^2\Omega_{3s}^2) = G_{13}^*/\overline{G_{13}} \tag{42}$$

Table 1. Material properties.

Property	Glass/Epoxy (V_f=52%)	Carbon/Epoxy (V_f=62%)	Glass/Epoxy (V_f=70%)
E_1 (MPa) undamaged	3620	13130	3800
E_2 (MPa) undamaged	8100	10800	11043
G_{12} (MPa) undamaged	3200	5200	5700
G_{13} (MPa) undamaged	1500	7100	4200
ν_{12} undamaged	0.23	0.29	0.24
F_{1t} (MPa)	932	2100	1220
F_{1c} (MPa)	370	1080	610
F_{2t} (MPa)	42	80	45
F_4 (MPa)	35	72	65
F_5 (MPa)	50	70	70
F_6 (MPa)	50	70	70
G_{12} (GPa) damaged	2700	2258	3876
G_{13} (GPa) damaged	1299	3083	2864
Numer of plies	16	20	29
Length (mm) L	100	122	250
Width (mm) w	36	25	80
Thickness (mm) t	6	2.5	10

which are the ratio between the damaged and the undamaged shear modulus for interlaminar shear, and substituting in Equations (38), (39), the following relationships hold

$$\sqrt{\frac{J_{22}r_{23}^S}{k_{23}^S} + \frac{J_{33}}{k_{23}^S r_{23}^S}\frac{2\overline{C_{44}}}{k_{23}^S}}F_4^2 = (\gamma + \gamma_0) = 1$$
$$\sqrt{\frac{J_{11}r_{13}^S}{k_{13}^S} + \frac{J_{33}}{k_{13}^S r_{13}^S}\frac{2\overline{C_{55}}}{k_{13}^S}}F_5^2 = (\gamma + \gamma_0) = 1 \tag{43}$$

In this way, the coefficients $(J_{33}, H_3, r_s^{13}, r_s^{23})$ can be obtained by solving the linear system defined by Equations (41) and (43). The only experimental data required are the interlaminar shear strength F_4 and F_5 and the damaged shear moduli G^*_{13} and G^*_{23} at imminent interlaminar failure, as shown in Table 1 from [8]. This completes the identification of the J and H tensors required for the definition of the damage domain.

NUMERICAL RESULTS AND DISCUSSION

The model results are now validated with experimental data available in the literature [8]. Predictions of in-plane damage only were already validated for different laminates in [6,23,24]. Interlaminar damage of a composite laminate is now investigated under torque loading conditions. The analysis is performed for three different polymeric matrix composite laminates. The available data are shown in Table 1 for different materials. The internal parameters shown in Table 2 define the shape of the damage and unrecoverable-deformation surfaces and the relative potentials. The in-plane and out-of-plane components of J and H tensors, which describe the shape of the damage evolution, and

Table 2. Model parameters determined explicitly from values in Table 1.

Property	Glass/Epoxy (V_f=52%)	Carbon/Epoxy (V_f=62%)	Glass/Epoxy (V_f=70%)
J_{11}	0.5310e-2	0.1897e-2	0.13129e-2
J_{22}	0.226	0.287e-1	0.3358
J_{33}	0.2009	0.534e-1	0.2144
H_1	0.6810e-1	0.2571e-1	0.1951e-1
H_2	−0.1445e-1	−0.807e-2	−0.1529e-1
H_3	0.592e-1	0.8018e-2	0.1803e-1
k_s^{13}	0.866	0.434	0.682
k_s^{12}	0.866	0.434	0.681
r_s^{12}	0.212	0.314	0.781
r_s^{13}	0.8703	0.311	0.924
r_s^{23}	4.105	0.992	1.179

Table 3. Adjustable parameters.

Property	Glass/Epoxy (V_f=52%)	Carbon/Epoxy (V_f=62%)	Glass/Epoxy (V_f=70%)
c_1	0.01	1	0.01
c_2	−0.0145	−1.10	−1.05E-1
γ_0	0	0	0

$r_{12}^S, r_{23}^S, r_{13}^S$, which express the ratio between damage on different planes, are used to write the model equations in a concise form. These are not adjustable model parameters since their values are univocally determined in terms of the available material constants F_{1t}, F_{1c}, F_{2t}, F_{2c}, and F_6. They are computed explicitly in terms of the values in Table 1 using Equations (41) and (43).

The parameters c_1^d, c_2^d, and γ_0 describe the evolution of the damage surface during a load increment. In particular c_1^d, c_2^d define the damage hardening law $\gamma(\delta)$ which is related to the damage increment. The damage threshold γ_0 represents the initial size of the damage surface. The values of the adjustable variables are identified (Table 2) using the in-plane shear stress–strain curve of a single composite lamina (Figure 1). The shear stress–strain curve for unidirectional polymer–matrix composites can be determined by a shear test as described in ASTM D5379, or from G_{12} and F_6 data using the hyperbolic tangent approximation described in [17,22].

A mesh sensitivity analysis was performed in order to choose an economic, yet accurate discretization. Rectangular samples were modeled by using the mesh shown in Figure 2. The length, width and thickness of the rectangular samples, denoted as L, w and t, respectively, are shown in Table 1. The end section displacements were fixed, but the longitudinal displacement is free to warp the section.

In order to show the effect of the interlaminar damage, the FEM case is first run with in-plane damage only (I.P.D), and then analysis is repeated with interlaminar damage.

Experimental data of torque versus twist-angle and acoustic emission counts for Glass/Epoxy (V_f=52%), are shown in Figure 3. The model yields good agreement with the experimental data and the interlaminar contributions are valuable. The curve labeled

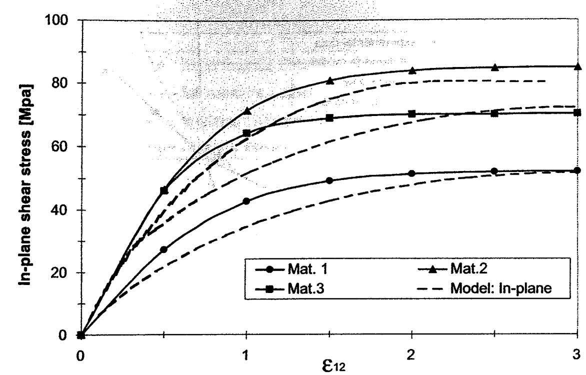

Figure 1. Adjusting in-plane behavior only (c_1^d, c_2^d, γ_0) with in-plane shear stress–strain data.

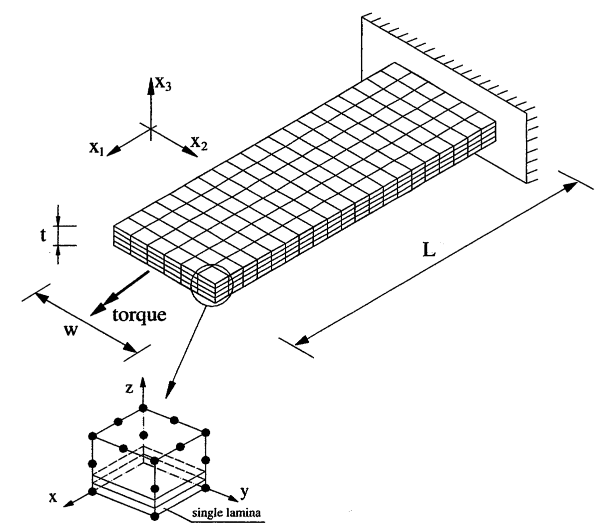

Figure 2. Mesh of the rectangular laminate under torque loading and detail of the 3-D layered isoparametric solid element.

"in-plane only" is obtained by turning off the interlaminar damage d_3. At the initial stages of the torque loading, the contribution of interlaminar damage is small and both prediction curves, "full-damage" and "in-plane only" are virtually identical. But for higher twist angle above 50°, interlaminar damage becomes important and the

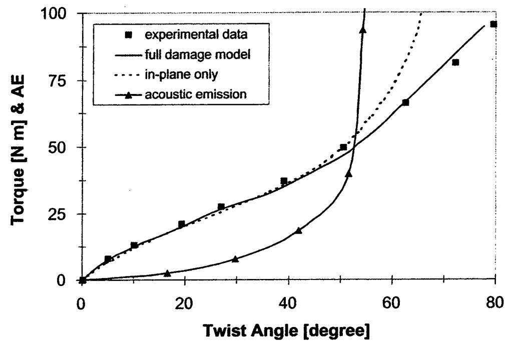

Figure 3. *Torque vs. twist-angle, material 1: glass-epoxy.*

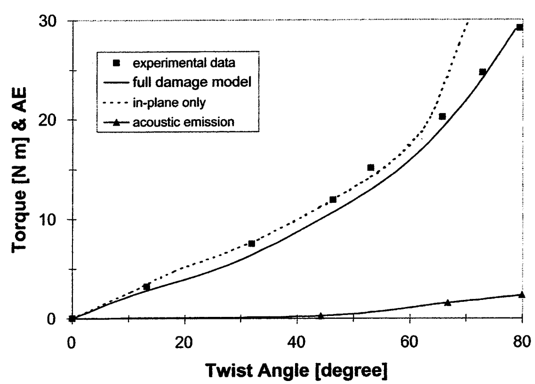

Figure 4. *Torque vs. twist-angle, material 2: carbon-epoxy.*

"in-plane only" prediction (dashed line) over-predicts the torque load drastically. Because of the aspect ratio $w/t = 6$ of the cross-section is high, warping is important, which leads to high interlaminar damage. In agreement with the model results, acoustic emissions are lower for the first part, and then increase rapidly [8].

Experimental data and model predictions for Carbon/Epoxy samples ($V_f = 62\%$) with aspect ratio $w/t = 4.88$ are shown in Figure 4. Due to the lower aspect ratio, which ensure low values of interlaminar stresses, the difference between "full damage" and "in-plane only" is less pronounced than in Figure 3 and any differences occur for larger twist angle, after 60°. This is consistent with the lower AE count reported [8].

Experimental data and model predictions for Glass/Epoxy ($V_f = 70\%$) samples with aspect ratio $w/t = 8$ are shown in Figure 5. The coupling behavior between the in-plane and interlaminar damage becomes important for small twist angle. Also, A.E. counts are

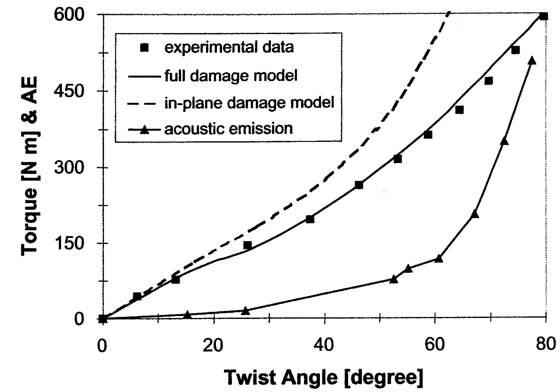

Figure 5. *Torque vs. twist-angle, material 3: glass-epoxy.*

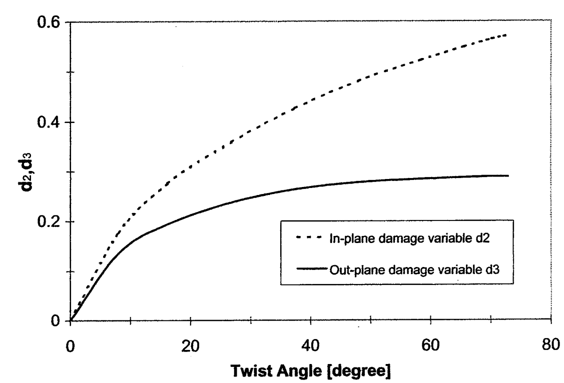

Figure 6. *In-plane and out-of-plane damage evolution material 3.*

significant at lower values of the twist angle and increase proportionally until a complete damaged condition [8].

Evolution of in-plane damage d_2 and interlaminar damage d_3 with increasing twist angle are shown in Figure 6. Interlaminar damage is significant, reaching close to the 50% of the in-plane value. As shown in Figure 6 the damage evolution curve reaches an asymptotic value, which corresponds to the critical damage value.

As shown in [8], high displacements in a torsion loading condition produce additional normal stresses, which are important for failure prediction. In order to further validate the model, axial stress (σ_{11}) across the half-width of the sample for various values of the twist angle are shown in Figures 7–9 for the three materials. The normal stresses are evaluated

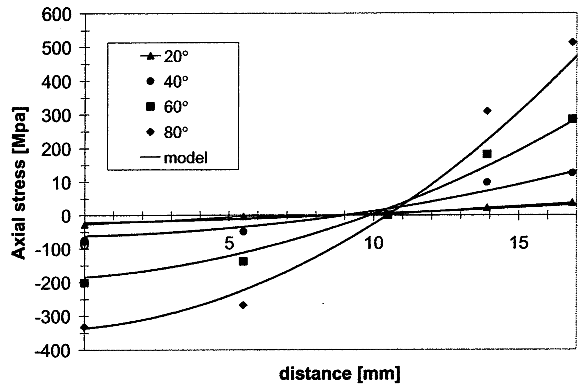

Figure 7. *Axial stress (σ_{11}) distribution as function of the twist angle material 1: glass-epoxy.*

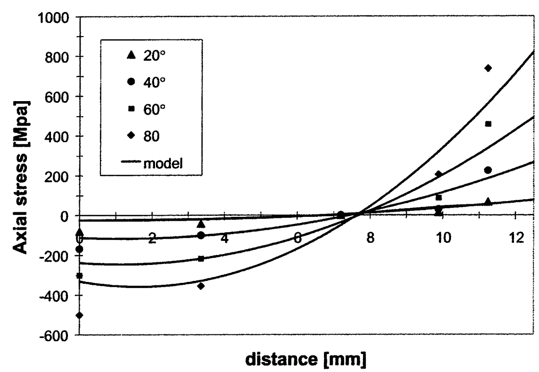

Figure 8. *Axial stress (σ_{11}) distribution as function of the twist angle material 2: carbon-epoxy.*

on the surface, at the midspan of the sample. All the curves pass through a zero longitudinal stress point, which separate the tension and compression zones. The comparison shows good agreement between the predicted and experimental results for the three materials.

CONCLUSIONS

A constitutive model is presented and implemented in a finite element formulation, in order to predict the damage evolution of a composite material laminate with in-plane and interlaminar damage. The theoretical model includes coupled damage and unrecoverable-deformations, in a consistent thermodynamic framework. A limited number of internal parameters are used in the model. All parameters are identified from experimental data available in the literature or easily obtained from standard tests. A generalization of the return-mapping algorithm for damage and unrecoverable deformation is presented in order to integrate the rate equations. The in-plane and interlaminar damage for three different types of materials are investigated, showing the influence of interlaminar damage in the presence of warping under torsion. The results show good agreement between the analytical and experimental results for the three materials.

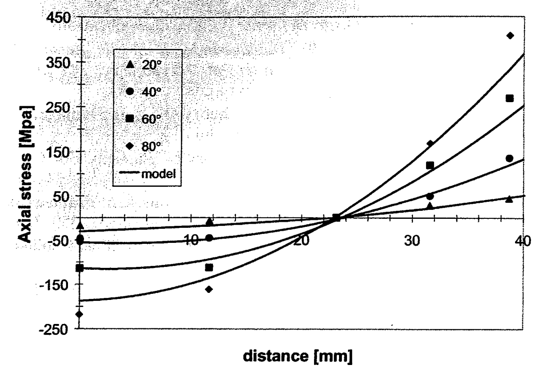

Figure 9. *Axial stress (σ_{11}) distribution as function of the twist angle material 3: glass-epoxy.*

REFERENCES

1. Krajcinovic, D. (1983). Constitutive Equations for Damaging Materials, *J. Appl. Mech.*, **50**: 355–360.
2. Murakami, S. (1988). Mechanical Modeling of Material Damage, *J. Appl. Mech.*, **55**: 281–286.
3. Chaboche, J.L. (1993). Development of CDM for Elastic Solids Sustaining Anisotropic and Unilateral Damage, *Int. J. of Damage Mechanics*, **v2**(4): 311–317.
4. Ladeveze, P. and LeDantec, E. (1992). Damage Modelling of the Elementary Ply for Laminated Composites, *Composites Science and Technology*, **v43**: 257–267.
5. Voyiadjis, G.Z. and Deliktas, B. (2000). A Coupled Anisotropic Damage Model For The Inelastic Response of Composite Materials, *Comp. Methods in Appl. Mech. Eng.*, **v183**: 159–199.
6. Barbero, E.J. and Lonetti, P. (2002). An Inelastic Damage Model for Fiber Reinforced Laminates, *Journal of Composite Material*, **36**(8): 941–962.
7. Lubliner, J. (1990). *Problems in Contained Plastic Deformation, Plasticity Theory*, Macmillan Publishing Company, New York, USA.
8. Gong, X.L., Laksimi, A., Lai, D.W. and Benzeggagh, M.L. (1995). Stress Analysis in Unidirectional Composite Plate under Torque Loadings: Experimental Observation, *Journal of Reinforced Plastic and Composite*, **14**: 2944.
9. Kachanov, L.M. (1958). On the Creep Fracture Time, Izv. *Akad Nauk USSR Otd. Tekh.*, **v8**: 26–31.
10. Kachanov, L.M. (1992). Effective Elastic Properties of Cracked Solids: Critical Review of Some Basic Concepts, *Appl. Mech. Rev.*, **v45**(8): 304–335.

11. Ogden, R.W. (1984). *Non-Linear Elastic Deformation*, Dover Publications, Inc., Mineola, NY.
12. Cordebois, J.L. and Sirodoff, F. (1979). *Damage-induced Elastic Anisotropy Mechanics of Behavior of Anisotropic Solids/N295 Comportement Mechanique Des Solides Anisotropes*, pp. 19–22, Martinus Nijhoff Publisher, The Netherlands.
13. Murakami, S. and Ohno N. (1981) A Continuum Theory of Creep Damage, In: Ponter, A.R.S. (ed.), *Creep in Structures*, pp. 422–444, Springer, Berlin.
14. Chow, C.L. and Wang, J. (1987) An Anisotropy Theory of Elasticity For Continuum Damage Mechanics, *Int. J. Fracture*, **v33**: 3–16.
15. Hansen, N. and Schreyer, H.L. (1994) A Thermodynamic Consistent Framework for Theories of Elastoplasticity Coupled With Damage, *Int. J. Solids Structures*, **v31**: 359–389.
16. Lubliner, J. (1972). On the thermodynamic foundations of nonlinear solids mechanics, *Int. J. Non-Linear Mech.*, **v7**: 237–254.
17. Barbero, E.J. (1999). *Introduction to Composite Materials Design*, Taylor & Francis, Philadelphia, PA.
18. Schwartz, M.M. (1997). *Composite Materials: Properties, Non-destructive Testing, and Repair*, Prentice Hall, NJ.
19. ASTM Standards (2000). *High Modulus Fibers and Composites*, **v15.03**.
20. Ju, J.W. (1988). On Energy-Based Coupled Elastoplastic Damage Theories: Constitutive Modeling and Computational Aspects, *Int. J. Solids Structures*, **25**(7): 803–833.
21. Owen, D.R. and Hinton, E. (1980). *Finite Element in Plasticity*, Pineridge Press Ltd, UK.
22. Barbero, E.J. and Tomblin, J. (1996). A Damage Mechanics model for Compression Strength of Composite, *Int. J. Solid Structures*, **33**(29): 4379–4393.
23. Barbero, E.J. and DeVivo, L. (2001). A Constitutive Model for Elastic Damage in Fiber-Reinforced PMC Laminae, *J. of Damage Mechanics*, **10**(1): 73–93.
24. Barbero, E.J. and Lonetti, P. (2001). Damage Model for Composites Defined in Terms of Available Data, *Mechanics of Composite Materials and Structures*, **8**(4): 299–316.
25. Mase, G.E. and Mase, G.T. (1992). *Continuum Mechanics for Engineers*, CRC Press, Boca Raton FL.
26. Herakovich, C.T. (1988). *Mechanics of Fibrous Composites*, John Wiley, N.Y.
27. Wen, E. (1999). Compressive Strength Prediction for Composite Unmanned Aerial Vehicles, Thesis, West Virginia University, Morgantown, WV.
28. Barbero, E.J. and Wen, E. (2000) Compressive Strength of Production Parts without Compression Testing, *ASTM STP 1383 Composite Structures: Theory and Practice*, pp. 470–483, ASTM, PA.
29. Piggott, M.R., Liu, K. and Wang, J. (2000). New Experiments Suggest that all the Shear and some Tensile Failure Processes are Inappropriate Subjects for ASTM Standards, *ASTM STP Composite Structures: Theory and Practice*.

Now published by SAGE Publications

Journal of Bioactive and Compatible Polymers

Editor **Raphael M. Ottenbrite** *Virginia Commonwealth University, USA*

...provides biomedical polymer scientists and researchers with new information on important advances in this field.

Coverage includes

- Advances in biomedical polymers: chemistry, performance, applications
- Original research reports by leaders in this field from around the world
- Applications in drug delivery including: controlled release, prodrugs, wound healing and other biomedical applications
- Special attention to new, novel and modified polymers
- Current Literature Reviews in each issue

Examples of specific areas of interest to the journal include: polymeric drugs and drug design; polymeric functionalization and structures related to biological activity or compatibility; natural polymer modification to achieve specific biological activity or compatibility; enzyme modelling by polymers; membranes for biological use; liposome stabilization and cell modeling.

Special feature

The journal also includes the bioactive and compatible polymers citation index containing citations of the current literature on bioactive and compatible polymers, and related subjects.

Six times a year: January, March, May, July, September, November.

ISSN: 0883-9115

SAGE Publications
6 Bonhill Street
London
EC2A 4PU, UK

SAGE Publications
2455 Teller Road
Thousand Oaks
CA 91320, USA

Order post-free visit www.sagepub.co.uk